Table 3 Representative pyrolysis product composition from the degradation of a 40% (by weight) Nylon-60% (by weight) phenolic resin ablative composite

Component	Mass percent	Mole percent
H_2	2.60	20.92
CH_4	3.87	3.90
C_2H_2	3.89	2.41
C_2H_4	3.90	2.24
C_2H_6	0.65	0.35
C_6H_6	2.59	0.53
C_6H_5OH	23.18	3.97
CO	4.18	2.40
CO_2	4.62	1.69
H_2O	7.21	6.45
N_2	3.83	2.20
Carbon (solid)	39.48	52.94
Total	100.00	100.00

Element	Mass percent	Mole percent
C	73.03	41.54
H	7.29	49.76
N	4.96	2.42
O	14.72	6.28
Total	100.00	100.00

this is comparable to the value of 146 Btu/lb experimentally measured by Sykes[2] and within the accuracy of the computations taking the residue to be carbon.

In summary, the comparison between the experimentally measured and computed heat of pyrolysis is within the accuracy of the data when a reasonably complete analysis of the pyrolysis products is available, i.e., when the higher molecular weight species such as phenol and other ring compounds from the degradation of phenolic resin are included.

Restricted equilibrium analysis

Restricted equilibrium analyses were made[14] for the degradation of a 40% (by weight) nylon-60% (by weight) phenolic resin composite using Eq. (1) as an additional constraint to free energy minimization calculations. The computations were done for two decomposition temperatures (600° and 700°C) because of the uncertainty involved in the physical properties used to calculate the average temperature, T_p. In addition, two different energy constraints (-228 and -390 Btu/lb of composite) were used because of uncertainties in the heat of pyrolysis.

In Table 2 a comparison is given for the preceding cases with chemical equilibrium and the experimental data of Sykes.[2] The computations and experiments show an order of magnitude agreement with the low molecular weight species. The agreement with the high molecular weight species of phenol, toluene, benzene, etc., was rather poor. Changing the energy constraint and the temperature did not cause any dramatic changes in the computed compositions. In general, restricted equilibrium provided an order of magnitude for the composition of low molecular weight compound. It failed to predict the composition of the higher molecular weight component.

A Representative Pyrolysis Gas Composition

Accurate compositions of the pyrolysis products are required for computations of the energy absorbed by a heat shield during entry. This is particularly true where radiation heating is a significant portion of the energy transferred to the surface of the ablator. The radiant energy transfer is particularly sensitive to the ablation products distribution in the shock layer. Thus based on the four methods discussed in this Note a representative composition of the pyrolysis products from the degradation of a 40% nylon-60% phenolic resin composite was estimated. This composition is given in Table 3, and it is consistent with the experimental data, the heat of pyrolysis analysis, and the molecular structure. It is also stoichiometrically consistent with the elemental composition of the composite.

References

[1] Madorski, S. L., *Thermal Degradation of Organic Polymers*, Interscience Publishing Co., New York, 1964, p. 262.

[2] Sykes, G. F., private communication, March 1969, NASA Langley Research Center, Hampton, Va.

[3] Sykes, G. F., "Decomposition Characteristics of a Char Forming Phenolic Polymer Used for Ablative Composites," TN D-3810, Feb. 1967, NASA.

[4] Nelson, J. B., "Determination of Kinetic Parameters of Six Ablative Polymers by Thermogravimetric Analysis," TN D-3919, April 1967, NASA.

[5] Friedman, H. L., "Pyrolysis of Plastic in a High Vacuum Arc Image Furnace," *Journal of Applied Polymer Science*, Vol. 9, 1965, pp. 1005–1018.

[6] Ladachi, M., Hamilton, J. V., and Cong, S. N., "Heat of Pyrolysis of Resins in Silica-Phenolic Ablators," *AIAA Journal*, Vol. 4, No. 10, Oct. 1966, p. 1798.

[7] Jackson, W. M. and Conley, R. T., "High Temperature Oxidative Degradation of Phenol-Formaldehyde Polycondensates," *Journal of Applied Polymer Science*, Vol. 8, 1964, pp. 2163–2193.

[8] Shulman, G. P. and Lochte, H. W., "Thermal Degradation of Polymers II. Mass Spectrometric Thermal Analysis of Phenol-Formaldehyde Polycondensates," *Journal of Applied Polymer Science*, Vol. 10, 1966, pp. 619–635.

[9] Pike, R. W., et al., "Comparison of Methods for Determining the Composition of Pyrolysis Products from the Degradation of Ablative Composites," NASA-RFL-9, Feb. 1970, Reacting Fluids Lab., Louisiana State Univ., Baton Rouge, La.

[10] Hougen, O. A., Watson, K. M., and Ragatz, R. A., *Chemical Process Principles Part I Material and Energy Balances*, 2nd ed., Wiley, New York, 1954, p. 297f.

[11] Parker, J. A. and Winkler, E. L., "The Effects of Molecular Structure on the Thermochemical Properties of Phenolics and Related Polymers," TR R-276, 1967, NASA.

[12] Gould, E. G., *Mechanisms and Structure in Organic Chemistry*, Holt, Rinehart, and Winston, New York, 1962, pp. 36–7.

[13] Swann, R. T., private communication, Nov. 1968, NASA Langley Research Center, Hampton, Va.

[14] del Valle, E. G. and Pike, R. W., "Computation of the Equilibrium Composition of Reacting, Gas-Solid Mixtures with Material and Energy Balance Constraints," NASA-RFL-10, March 1970, Reacting Fluids Lab., Louisiana State Univ., Baton Rouge, La.

Effect of Gas Composition on the Ablation Performance of Phenolic Nylon

JOHN J. BERTIN,* MICHAEL J. NIPPER,† AND
WILLIAM D. CONINE‡
University of Texas at Austin, Texas

A NUMBER of recent experimental investigations[1–6] have considered the removal of surface char from the stagnation region of phenolic-nylon specimens exposed to high-temperature, arc-heated gas streams. The surface-

---

Presented as Paper 70-154 at the AIAA 8th Aerospace Sciences Meeting, New York, January 19–21, 1970; submitted May 13, 1970; revision received June 29, 1970.

* Assistant Professor, Department of Aerospace Engineering and Engineering Mechanics, University of Texas at Austin. Member AIAA.

† Research Assistant; presently Lieutenant, U.S. Marine Corps.

‡ Research Assistant; presently Engineer/Scientist, TRACOR, Inc., Austin, Texas.

Table 1 Average test-stream measurements

Condition	Gas	P_s, 10^{-4} atm	$\dot{q}_{cw}$, Btu/ft^2-sec	$\bar{H}$, Btu/lb	H_{cl}, Btu/lb
1	N_2	62	97	4520	7690
2	N_2	91	157	5720	10780
3	N_2	135	102	2720	3800
4	N_2	171	192	3090	4320
5	N_2	221	385	7640	11530
6	N_2	241	289	5580	7420
7	N_2	445	283	4660	4850
8	Air	68	89	4400	8020
9	Air	97	174	6400	11170
10	Air	164	112	2690	3690
11	Air	227	395	6240	10290
12	Air	242	294	4840	7540
13	Air	270	196	3770	4450
14	Air	445	289	4740	5050
15	N_2/CO_2	78	102	5680	9920
16	N_2/CO_2	89	155	6730	11830
17	N_2/CO_2	145	108	2420	3420
18	N_2/CO_2	239	270	5000	7270
19	N_2/CO_2	260	96	3620	4070
20	N_2/CO_2	443	285	4910	5340
21	N_2/CO_2	594	569	6350	8970

recession velocities measured in air[7] compared favorably with the values calculated using the relation of Scala and Gilbert[8] for diffusion-limited oxidation of graphite in air.

This note provides data on the ablative performance of low-density phenolic nylon in an inert stream (N_2), in simulated air (0.80 N_2, 0.20 O_2 by volume), and in a planetary atmosphere (0.60 N_2, 0.40 CO_2 by volume).

The tests, conducted in the Hyperthermal Tunnel of the University of Texas at Austin, include model stagnation pressures from 0.006 to 0.06 atm with stagnation enthalpies from 3000 to 12,000 Btu/lb. The 80-kw dc, continuous flow, plasma arc-tunnel can provide either a 1.5-in. or 3.0-in.-diam stream of a two-component gas at a nominal Mach number of 3. The data, averaged over all the runs of a nominal flow condition, are presented in Table 1. Included is the model stagnation pressure P_s, the cold-wall stagnation-point heat-transfer rate $\dot{q}_{cw}$, the average total enthalpy at the nozzle exit $\bar{H}$, and the centerline enthalpy H_{cl}. These average values were usually within 3% of the extreme values associated with a nominal condition.

The models were machined from low-density phenolic nylon, which was 50% (by weight) powdered nylon, 25% phenolic resin, and 25% phenolic microballoons, and had a nominal density of 35.0 lb/ft^3 (the densities of individual model cores varied from 33.7 to 36.8 lb/ft^3). The model configuration was a 1.00-in.-diam, flat-faced cylinder with a 0.50-in.-diam concentric core. The interface velocities were calculated with a linear least-squares-curve fit of the experimental interface-location histories. The total mass-loss rate $\dot{m}_t$ and the pyrolysis mass-loss rate $\dot{m}_p$ were computed in a similar manner. Table 2 shows that $\dot{m}_p > \dot{m}_t$ for each test condition; this behavior is referred to as quasi-steady-state ablation, as opposed to steady-state ablation where $\dot{m}_p = \dot{m}_t$.

Several additional mass-loss rates were computed. The char-removal rate was calculated using the surface velocity and the average char density:

$$\dot{m}_{cr} = \bar{\rho}_c V_s \tag{1}$$

The char-production rate was calculated as the product of the char/pyrolysis interface velocity and the average char density:

$$\dot{m}_{cp} = \bar{\rho}_c V_c \tag{2}$$

The average char density was 15.3 lb/ft^3, with extreme values of 13.4 and 17.5 lb/ft^3. There was a tendency for the longer chars to have a slightly higher density. This may be an indication of coking, i.e., deposition of carbon in the char matrix due to reactions of the pyrolysis gases as they percolate to the surface.

The vapor-production rate $\dot{m}_{vp}$ was calculated by two methods. From the definition that the total mass-loss rate $\dot{m}_t$ is the sum of $\dot{m}_{vp}$ and $\dot{m}_{cr}$, we have

$$\dot{m}_{vp} = \dot{m}_t - \dot{m}_{cr} \tag{3}$$

and from the definition that the pyrolysis mass-loss rate is the sum of the vapor-production rate and char-production rate,

$$\dot{m}_{vp} = \dot{m}_p - \dot{m}_{cp} \tag{4}$$

These two methods of calculating $\dot{m}_{vp}$ are generally in good agreement (Table 2).

Analysis and Discussion of Results

Surface recession of a charring ablator can result from sublimation, shrinkage, shear stress, reactions with boundary-layer species (from the test stream), and reactions with the pyrolysis gases. According to Lundell,[2] sublimation of phenolic-nylon char does not occur in a vacuum until a temperature of 5550°R is reached and at even higher temperatures at higher pressures. Therefore, sublimation was not considered to occur for the present conditions. Aerodynamic shearing effects were assumed negligibly small, since the model cores were in a stagnation region and even the corners of the concentric sleeve (where shear stresses would be greatest) remained sharp during the run.

Tests in nitrogen

The surface recession velocities (V_s's) and char/pyrolysis interface velocities (V_c's) observed in nitrogen, and for radiative heating in a vacuum, are plotted vs T_s in Fig. 1. Although the P_s's differed by a factor of two, the V_s's at 4400°R are approximately equal for the two points from the present program. Thus, it is concluded that the V_s in nitrogen depends only on T_s. The curves faired through the present data merely indicate the relation between V_s and T_s. The surface recessions observed in the "inert" nitrogen environment are attributed to shrinkage and surface reactions with pyrolysis gases.

Table 2 Loss rates, 10^{-5} lb/ft^2-sec

Condition	$\dot{m}_t$	$\dot{m}_p$	$\dot{m}_{cr}$	$\dot{m}_{cp}$	$\dot{m}_{vp}$[a]	$\dot{m}_{vp}$[b]
1	592	780	81	239	511	541
2	741	936	89	350	652	586
3	570	704[c]	118	262	452	442
4	687	968	124	402	563	566
5	1204	1730	210	707	994	1023
6	1111	1551	182	641	929	910
7	938	1357	185	606	753	751
8	714	876	179	297	535	579
9	851	1025	200	488	651	537
10	746	885	303	387	443	498
11	1758	1977	350	565	1412	1408
12	1176	1479	343	621	833	858
13	1255	1538	349	603	906	935
14	1603	1898	539	874	1064	1024
15	915	1124[c]	132	416	783	708
16	959	1224	179	456	780	768
17	731	822	179	277	552	545
18	1050	1221	259	496	791	725
19	1091	1271[c]	243	487	848	784
20	1473	1756	427	785	1046	971
21	1499	2059	471	880	1028	1179

[a] Calculated using Eq. (3).
[b] Calculated using Eq. (4).
[c] Calculated using $\rho m V p$ (where ρm is the density of the virgin material, Vp the velocity of the pyrolysis/virgin material interface).

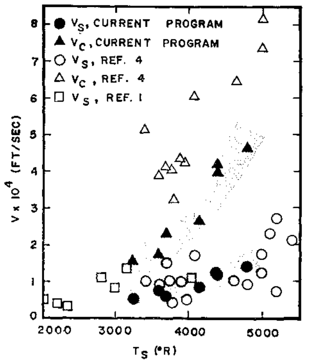

Fig. 1 Velocities in "inert" streams.

Tests in air and in N_2/CO_2

In streams of air and of N_2/CO_2, combustion with gases present in the boundary layer constitutes a principal cause of surface recession for a phenolic-nylon char. Since the phenolic-nylon char is principally carbon,[9] the data are compared with the theoretical relation of Scala and Gilbert.[8] The present range of test conditions, i.e., $P_s \geq 0.006$ atm and $3000 \leq T_s \leq 5000°$R, falls within the diffusion-controlled regime for the combustion of graphite in air. Scala and Gilbert developed the following expression for the diffusion-limited oxidation rate of graphite in air:

$$\dot{m}_G = 0.00635(P_s/R_{\text{eff}})^{0.5} \tag{5}$$

where R_{eff} is the effective nose radius of the model. Assuming the char removal at the surface of the ablative material can be approximated by the graphite model, the surface velocity V_s may be calculated using the expression

$$\begin{aligned} V_s &= (0.00635/\bar{\rho}_c)(P_s/R_{\text{eff}})^{0.5} \\ &= 0.000415(P_s/R_{\text{eff}})^{0.5} \end{aligned} \tag{6}$$

The V_s measurements of the current program and of Lundell et al.[4] are compared in Fig. 2 with the values predicted by Eq. (6). For the present tests, the effective nose radius was assumed to be 2.9 R_b, where R_b is the model body radius. The surface-recession velocities in N_2/CO_2 were slightly less than those observed in air and significantly higher than those observed in the "inert" N_2 environment. Thus, the data indicate significant amounts of oxygen can be released from the dissociation of the CO_2, as much as 40% O and O_2 by volume in equilibrium.[10] For the air and the N_2/CO_2 streams, $V_s \propto P_s^{0.5}$. Thus, the combustion of the char in these two environments was assumed to be diffusion-limited. In Fig. 3 the char-removal parameter, $\dot{m}_{cr}(R_{\text{eff}}/P_s)^{0.5}$ (which represents the surface velocity with the theoretical pressure dependence removed) is plotted vs T_s. Included in the upper part are air data from Ref. 1 and a line representing the diffusion-limited theory of Scala and Gilbert, for which the surface-removal parameter is independent of temperature. No dependence on T_s is observed for the air data, but the measurements in N_2/CO_2 depend slightly on T_s, possibly due to increased reactivity between CO_2 and C to form CO at elevated temperatures.

For a char-forming ablation material, the V_s caused by oxidation would be expected to be less than that for a graphite model, since ablation vapors (i.e., pyrolysis gases and surface reaction products) reduce the amount of oxygen diffusing to the surface by physical blockage and by chemical consumption in gas-phase reactions. The surface velocities measured in air and in N_2/CO_2 streams and presented in Figs. 2 and 3 are comparable to the theoretical values for oxidation of graphite. However, these V_s measurements include contributions caused by shrinkage and surface removal because of reactions with the pyrolysis gases. The results of the nitrogen tests show that these two factors produce a surface velocity which is 30% of the char-interface velocity. Assuming the same relative inert effects are present in the other environments, the increment of surface velocity due to oxidation ΔV_s may be approximated by

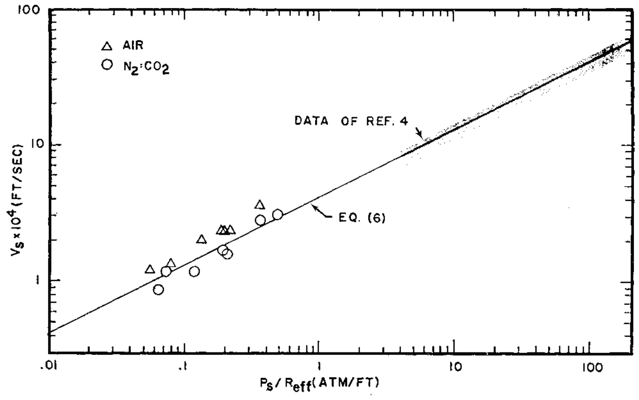

Fig. 2 Comparison of surface velocities.

$$\Delta V_s = V_s - 0.3V_c \tag{7}$$

The corresponding char-oxidation rate is then given as

$$\Delta\dot{m}_{cr} = \bar{\rho}_c \Delta V_s = \bar{\rho}_c (V_s - 0.3V_c) \tag{8}$$

The char-oxidation parameter, determined using Eq. (8) with the degradation measurements obtained in air and in N_2/CO_2 streams, is plotted vs T_s in the lower part of Fig. 3. The ratio of the vapor-injection rate to the char-oxidation rate, $\dot{m}_{vp}/\Delta\dot{m}_{cr}$, is indicated for each data point. It can be seen from the data that the char-oxidation parameter decreases as $\dot{m}_{vp}/\Delta\dot{m}_{cr}$ increases. Therefore, $\dot{m}_{cr}$ for the char-forming ablation material depends not only upon P_s but also the pyrolysis-gas injection rate both for air and for N_2/CO_2

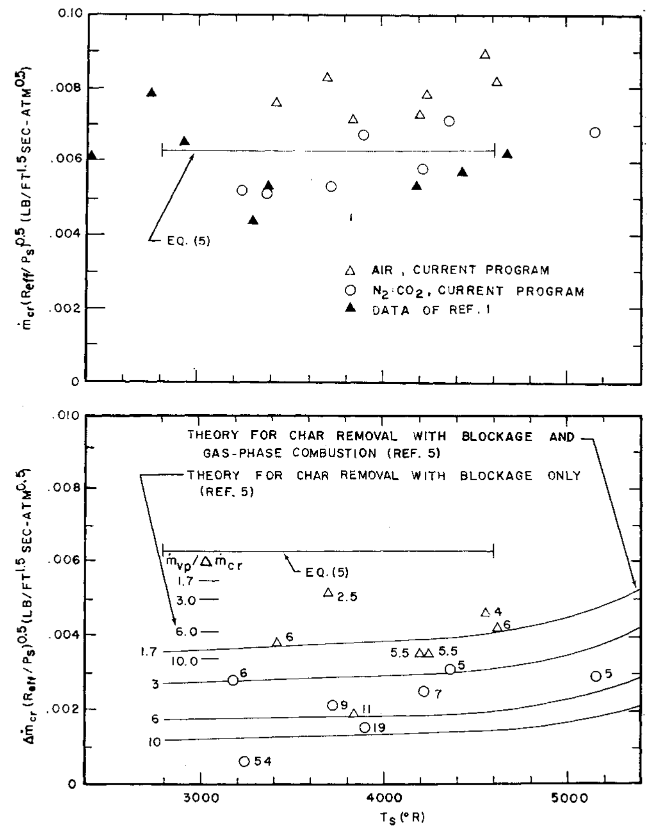

Fig. 3 Comparison of char-removal parameter; bottom, effect of pyrolysis gas injection on the char-oxidation parameter.

streams. Thus, the data clearly indicate the effects of pyrolysis-gas injection, i.e., blockage and consumption of boundary-layer oxygen in gas-phase chemical reactions.

Included in the lower part of Fig. 3 are the theoretical correlations for the char-removal parameter in air for a low-density phenolic-nylon composite as presented in Wakefield et al.[5] Theoretical relations were obtained assuming 1) an analytical model with diffusion blockage, but without gas-phase chemical reactions; and 2) a model which included the influence of chemical reactions between the pyrolysis gases and the stream species in addition to the blockage effect. To perform these calculations for a particular case, the elemental compositions of the stream, pyrolysis gases, and surface char were specified to match the experimental program of Ref. 5. The data from the present program, which exhibit the expected variation with $\dot{m}_{vp}/\Delta\dot{m}_{cr}$, fall beween the char-removal rates predicted using the two theoretical correlation models. The lack of better quantitative agreement with the theory for a reactive pyrolysis gas is attributed to differences in materials and in the flow conditions of the present tests and those of Ref. 5.

Comparative performance in the three environments

The external degradation parameter, i.e., surface recession, indicates that air is the most severe environment, followed closely by N_2/CO_2, with inert N_2 the least severe. The rate of internal degradation of a phenolic-nylon material depends only upon the in-depth temperature profile. As discussed by Parker and Winkler,[11] the degradation process itself is anaerobic and independent of the mode of heating. Further, except possibly at very high stagnation pressures and low heating rates, the pyrolysis gas flow prevents the boundary-layer gases from penetrating the surface due to the very high pressures generated in the decomposition zone. However, the composition of the external environment is an important factor in the internal degradation process, since the chemical reactions at the surface and in the boundary layer determine the thickness of char layer and, to some degree, the surface temperature. Since the temperature at the char/pyrolysis interface depends on the degradation properties of the material and is usually assumed to be a constant, the thermal gradient (and, hence, the rate at which energy is supplied to the pyrolysis zone) across the char is dependent upon the composition of the external environment.

If one considers the data from those tests with comparable flow conditions, one finds an effect of gas composition. For tests with different gas compositions to be considered as comparable flow conditions, it was necessary that H_{Ci} and P_s be approximately equal. Using these criteria, conditions 1 and 8, 3 and 10, 12 and 18, and 7, 14, and 20 provide material performance data at comparable conditions.

The internal interface velocities in air were generally about 30% higher than those in N_2 and about 15% higher than those in N_2/CO_2, even though the surface temperatures in air were only slightly higher (100–170°F) than in N_2. The surface temperatures in the N_2/CO_2 mixture were similar to those observed in the other two streams. Further analysis of the data indicates that the differences between the internal degradation rates measured in air and those measured in nitrogen streams become more pronounced with increasing stagnation pressure. This dependence on pressure is believed to reflect the effects of surface combustion. First, the exothermic surface combustion increases heating to the surface and, since the increased char removal results in a thinner char cap, the thermal gradient across the char cap is larger. Both factors contribute to a higher rate of conduction of energy across the char layer to supply the degradation process.

References

[1] Vojvodich, N. S. and Pope, R. B., "Effect of Gas Composition on the Ablation Behavior of a Charring Material," *AIAA Journal,* Vol. 2, No. 3, March 1964, pp. 536–542.

[2] Lundell, J. H., Wakefield, R. M., and Jones, J. W., "Experimental Investigation of a Charring Ablative Material Exposed to Combined Convective and Radiative Heating," *AIAA Journal,* Vol. 3, No. 11, Nov. 1965, pp. 2087–2095.

[3] Clark, R. K., "Effect of Environmental Parameters on the Performance of Low-Density Silicone-Resin and Phenolic-Nylon Ablation Materials," TND-2543, Jan. 1965, NASA.

[4] Lundell, J. H., Dickey, R. R., and Jones, J. W., "Performance of Charring Ablative Materials In The Diffusion-Controlled Surface Combustion Regime," *AIAA Journal,* Vol. 6, No. 6, June 1968, pp. 1118–1126.

[5] Wakefield, R. M., Lundell, J. H., and Dickey, R. R., "Effects of Pyrolysis-Gas Chemical Reactions on Surface Recession of Charring Ablators," *Journal of Spacecraft and Rockets,* Vol. 6, No. 2, Feb. 1969, pp. 122–128.

[6] McLain, A. G., Sutton, K., and Walberg, G. D., "Experimental and Theoretical Investigation of the Ablative Performance of Five Phenolic-Nylon-Based Materials," TN D-4374, April 1968, NASA.

[7] Bertin, J. J., Conine, W. D., and Nipper, M. J., "Surface Recession of Phenolic Nylon in Low-Density Arc-Heated Air," *AIAA Journal,* Vol. 7, No. 11, Nov. 1969, pp. 2163–2165.

[8] Scala, S. M. and Gilbert, L. M., "Sublimation of Graphite at Hypersonic Speeds," *AIAA Journal,* Vol. 3, No. 9, Sept. 1965, pp. 1635–1644.

[9] Kratsch, K. M., Hearne, L. F., and McChesney, H. R., "Theory for the Thermophysical Performance of Charring Organic Heat-Shield Composites," Rept. 803099, Oct. 1963, Lockheed Missiles and Space Co., Sunnyvale, Calif.

[10] Baily, H. E., *Equilibrium Thermodynamic Properties of Three Engineering Models of the Martian Atmosphere,* SP-3021, NASA, 1965.

[11] Parker, J. A. and Winkler, E. L., "The Effects of Molecular Structure on the Thermophysical Properties of Phenolics and Related Polymers," TR R-276, Nov. 1967, NASA.

Thermal Curvature Time Constants of Thin-Walled Tubular Spacecraft Booms

F. R. Vigneron*
Communications Research Center, Department of Communications, Ottawa, Canada

SEVERAL "time constants" associated with thin-walled tubular spacecraft booms have arisen in astrodynamics applications: one for average temperature rise after the boom emerges from shadow into sun, another associated with thermal flutter, another associated with the establishment of thermal curvature resulting from a solar step function input, and, as will be seen, yet another associated with thermal curvature resulting from a periodically varying input such as is experienced by a boom rotating end over end in the ecliptic plane. These constants are interrelated, but they all have different quantitative values; this Note addresses the latter two, which are important to the development of theories of solar-induced despin of the Alouette and ISIS satellites.[1,2] In developing a solar despin theory, Etkin and Hughes hypothesized that solar induced curvature would be governed by a first-order linear equation of the form,

$$[\partial\kappa_T(x,t)/\partial t] + (1/T)\kappa(x,t) = f(x,t) \qquad (1)$$

where $\kappa_T(x,t)$ is the thermally induced curvature, x is the length coordinate of the boom, t is time, $f(x,t)$ is an external radiation input, and T is a thermal time constant. No particular restrictions were placed on the range of application of the

---

Received June 10, 1970; revision received July 30, 1970.

* Research Scientist, National Space Telecommunications Laboratory.